arXiv:1401.5643v1 [physics.atom-ph] 22 Jan 2014

Hole burning and higher order photon effects in attosecond light-atom interaction

P. L. Price[1],* L. D. Noordam[2], H. B. van Linden van den Heuvell[2], and F. Robicheaux[1†]
[1]*Department of Physics, Auburn University, AL 36849, USA and*
[2]*Institute of Physics, University of Amsterdam, PO Box 94485, 1090GL Amsterdam, The Netherlands*
(Dated: January 23, 2014)

We have performed calculations of attosecond laser-atom interactions for laser intensities where interesting two and three photon effects become relevant. In particular, we examine the case of "hole burning" in the initial orbital. Hole burning is present when the laser pulse duration is shorter than the classical radial period because the electron preferentially absorbs the photon near the nucleus. We also examine how 3 photon Raman process can lead to a time delay in the outgoing electron for the energy near one photon absorption. For excitation out of the hydrogen $2s$ state, an intensity of 2.2×10^{16} W/cm^2 leads to a 6 attosecond delay of the outgoing electron. We argue that this delay is due to the hole burning in the initial state.

PACS numbers: 78.47.J-, 32.80.Fb, 32.80.Rm

I. INTRODUCTION

The past several decades have witnessed the increase in the speed of lasers as tracked by the duration of a laser pulse. In recent years, experimental groups have been able to decrease this duration into the attosecond regime.[1] With each decrease in duration of the laser pulse, it is possible to probe quantum systems on shorter time scales. For example, there have been many recent measurements and calculations of the delay in the photoionization of electrons from atoms.[2–5] This example is interesting in that the delay is only of order 10 as but can be measured using a streaking IR field *and* that measurements and calculations differ in the expected delay; the reason for the difference is not clarified. One of the results we discuss below is that delays in electron ejection naturally occur at higher laser intensities.

Although both the laser frequency and duration determine what types of systems and phenomena are best investigated, there are types of processes whose similarities extend from the attosecond to the picosecond regime. One of the processes that spans a broad regime is that a short laser pulse can burn a hole in a wave function. The reason is that photoabsorption is often highly position dependent. For example, stationary phase considerations lead to the realization that photo-ionization occurs near the nucleus within a region $r \sim \sqrt{(\ell+1)/\omega}$ with ω being the angular frequency of the laser.[6] Thus, a laser pulse that is shorter than the radial period of the electron can deplete the wave function in the neighborhood of the nucleus.[9]

Figure 1 is a schematic of two photon processes. The gray bands are meant to indicate the spread in energy for the processes that arise from the short duration of the laser. The dark arrow is the one photon excitation step. The narrow solid arrows are the two photon absorption (for increasing energy) and the Raman process (for decreasing energy). The Raman process back to $\ell = 0$ gives the hole burning of the initial wave function. The dashed arrows indicate three photon process that can interfere with the one photon absorption; the three photon processes can modify both the energy distribution and the ejection time of the electron.

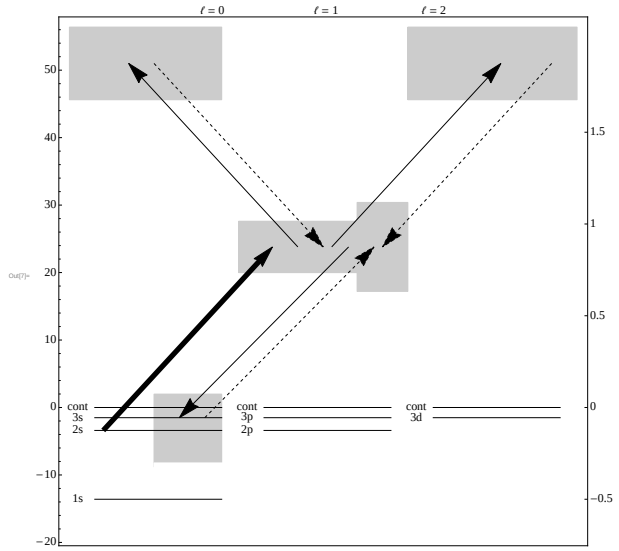

FIG. 1: A schematic drawing of the energy levels and transitions described in the paper.

Hole burning was investigated in Rydberg states where the radial period can be in the picosecond regime.[7, 8] For a state with energy $E = -1/2\nu^2$, the radial period is given by $T_{Ryd} = 2\pi\nu^3$ a.u. which is $T_{Ryd} = 1.52 \times 10^{-4}\nu^3$ ps. Thus, states with $\nu > 18.7$ have periods longer than a picosecond. One of the manifestations of hole burning is Raman transitions to nearby states with the same ℓ. One way to think of this connection is that the wave function with the hole, ψ_h, is

*Now at Physics Department, University of Connecticut, 2152 Hillside Rd., Storrs Connecticut 06269-3046, USA
†Now at Department of Physics, Purdue University, West Lafayette, Indiana 47907, USA; Electronic address: robichf@purdue.edu

projected onto the eigenstates with the laser off. Since the ψ_h mostly resembles the initial state and has the same angular momentum, the projection onto the initial state and states with small change in ν and no change in ℓ will be emphasized.[9] The size of the hole in space increases with the duration of the laser pulse. Thus, a short laser pulse will lead to a wider energy range of final states. An equivalent statement in the frequency domain is that short pulses have a large bandwidth, supporting Raman transfer to neighbouring states.

In this paper, we examine the phenomenon of hole burning in the regime of attosecond laser pulses. Since hole burning is at least a two photon process, the intensity regime will be higher than what is currently experimentally achieved but not so high that experiments are unthinkable. While the basic phenomenon of hole burning should be the same, there are differences due to the shorter time scale and hence the lower states involved. One difference is that for Rydberg states and picosecond lasers, the hole burning leads to population at both higher and lower energies (the principle quantum number can both increase or decrease) while for attosecond lasers the initial state is usually the ground state so population can only transfer to higher energies. Another difference is that the experiments on Rydberg state hole burning did not investigate when the *ejected* electron is modified by the hole burning. In attosecond physics, the time delay of the ejected electron is often one of the more interesting parts of the measurement but also used to define the 'zero' time delay in pump-probe experiments. We give calculations for this process and show that the hole burning leads to a delay in the ejection of the electron. This effect arises from the interference between one photon absorption and a three photon process (2 absorptions and one emission).

We use atomic units unless SI units are explicitly given.

II. NUMERICAL METHOD

We solved the time dependent Schrödinger equation by representing the wave function on a grid of radial points and an angular momentum basis. A more extensive discussion of the technique can be found in Ref. [10]. In our calculations, we used linearly polarized light which leads to a wave function that can be represented by the summation

$$\Psi(\vec{r}) = \sum_{\ell} [R_\ell(r,t)] Y_{\ell m}(\Omega) \tag{1}$$

where the radial functions, R_ℓ, contain all of the useful information about the wave function. The maximum ℓ in the sum is determined by the duration, strength and frequency of the laser and was chosen so that less than 10^{-9} of the population was in ℓ_{max}. For ease in solving the time dependent Schrödinger equation, we consider the Hamiltonian for this calculation as the sum of two terms:

$$H = H_1 + H_2 = H_{atom} + H_{field} \tag{2}$$

where H_1 is the atomic Hamiltonian which contains the kinetic energy operator and the spherical potential from the electron-ion interaction and the H_2 is the laser-electron interaction. For hydrogen, the electron-ion potential is simply $-1/r$. For the other atoms presented in this paper, a model potential can be used.

The Hamiltonian for the laser field was taken to be in the length gauge. We do not need to worry about the increasing size of the laser potential with r because the laser duration is so short the electron does not travel far before the laser intensity returns to 0. We chose $H_2 = zE(t)$ where $E(t) = -dA/dt$ with

$$A(t) = F(t)\frac{1}{\omega_0}\sin(\omega_0 t + \phi). \tag{3}$$

The ϕ is the carrier envelope phase and $F(t)$ is a smooth function giving the envelope. We chose this to be a Gaussian $F(t) = F_{max}\exp(-t^2/t_w^2)$ with F_{max} the maximum electric field when the carrier envelope phase is zero.

We used a split operator method with a Crank-Nicolson approximation to step the wave function by δt. The approximation is

$$\Psi(t+\delta t/2) = U_2(t,\delta t/2)U_1(\delta t)U_2(t,\delta t/2)\Psi(t-\delta t/2) \tag{4}$$

where the

$$U_j(t,\delta t) = [1 - iH_j(t)\delta t/2][1 + iH_j(t)\delta t/2]^{-1} \tag{5}$$

gives $O(\delta t^3)$ accuracy for one time step. In the propagator, we only need to perform the U_2 when $|t| < 6t_w$ because H_2 is approximately 0 outside of that range. Both the H_1 and H_2 operators can be represented as tridiagonal matrices. For the electric field, the operator H_2 only couples ℓ to $\ell \pm 1$. We used two approximations for H_1, both of which gives a tridiagonal representation, as a test of convergence. In the simplest approximation, we used equally spaced points in r (i.e. $r_j = j\delta r$) and a three point difference for the radial kinetic energy. The more complicated approximation used a square root mesh and a Numerov approximation as in Ref. [11]. In all calculations, we checked convergence with respect to the number of radial points, the number of angular momenta, and the number of time steps.

Before the laser turns on, the wave function is in an eigenstate. We find the eigenstate by diagonalizing H_1 in a finite region $r < r_{max}$. The r_{max} is chosen to be large enough that the wave function can not reach that distance while the laser is on. We also used the eigenstates of H_1 to compute the energy distribution of the final state. The eigenstates go to 0 at r_{max} which leads to a discretized continuum. The energy distribution with angular momentum ℓ is approximated by

$$P_\ell(\bar{E}) = \frac{|<a+1,\ell|\Psi>|^2 + |<a,\ell|\Psi>|^2}{2(E_{a+1,\ell} - E_{a,\ell})} \tag{6}$$

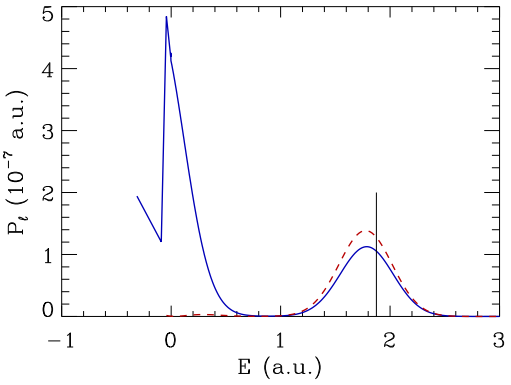

FIG. 2: The energy distribution in atomic units of electrons for $\ell = 0$ (solid line) and $\ell = 2$ (dashed line). In this calculation, we set $\omega = 1$, $F_{max} = 0.05$ a.u. and $t_w = 6.0$ a.u. In the energy distribution formula, we set the population of the 2s state to 0. The peak just below 2 a.u. is from two photon absorption; the vertical line marks the position where a narrow band laser would have the two photon ATI peak. The Raman feature is from approximately -0.2 to 0.8 a.u. The $\ell = 2$ Raman transition is very weak and is hardly visible on the graph. The $\ell = 0$ Raman structure is associated with hole burning in the initial state.

where $E_{a,\ell}$ is the energy of the a-th eigenstate with angular momentum ℓ, $\bar{E} = (E_{a+1,\ell} + E_{a,\ell})/2$ is the average of the two energies, and $< a, \ell|\Psi >$ is the projection of that eigenstate on the wave function. We also use this definition for negative energy states which allows us to treat both positive and negative energy on the same curve. This has the disadvantage that it is not clear what is the population in an individual state, which is a measurable quantity.

III. TWO-PHOTON PROCESSES

In this section, we present results on two photon ionization and on one photon absorption followed by one photon emission (and vice versa). We investigate the latter process in more detail because it is the mechanism that leads to "hole burning" of the initial orbital.[7] It is important to remember that even a weak laser pulse whose time width is shorter than the Rydberg period will burn a hole in the wavefunction. The depth of the hole increases with laser intensity and, for weak fields, the result of the hole burning will scale with the square of the intensity. However, the states described in this section are not populated by other mechanisms and, thus, can be distinguished even for weak lasers.

Figure 2 shows the energy distribution in atomic units for the 2-photon processes when starting from the 2s state of H. For the presentation of the energy distribution, we set the population in the 2s to 0 when using Eq. (6) because we want a plot of what states gained population; this choice leads to an artificial dip in the Raman process. The solid line is the energy distribution where the electron has $\ell = 0$ and the dashed curve is for $\ell = 2$. In this calculation, we set $\omega = 1$ (= 27.2 eV, $\lambda = 45.6$ nm), $F_{max} = 0.05$ a.u. and $t_w = 6.0$ a.u. The full width at half maximum (FWHM) of the laser intensity is $t_{FWHM} = \sqrt{2 \ln 2} t_w$ which corresponds to 170 as in this calculation. The electric field corresponds to a maximum laser intensity of 8.8×10^{13} W/cm^2 which is in the perturbative regime. Doubling the intensity increases the scale of Fig. 2 by a factor of 4. For this laser width, the state with the most population is the $1s$ state; this is not obvious in Fig. 2 due to the large energy difference between the $1s$ and $2s$ states which gives a large denominator in Eq. (6).

There are a few features worth noting in Fig. 2. The two photon absorption peak is at nearly the same energy for the two angular momenta. However, this energy, 1.78 a.u., is *not* at the expected energy for two photon absorption which is $-1/8 + 2 = 1.875$ a.u.; the expected energy is marked by a vertical line in the graph. The peak is shifted down in energy because the two photon absorption amplitude is a decreasing function of energy; the product of the decreasing absorption amplitude and the Gaussian centered at 1.875 a.u. gives the approximately 0.09 a.u. shift. Using a longer laser pulse, leads to this feature becoming narrower in energy with the peak shifting toward the expected value of 1.875 a.u. For example, the peak shifts to 1.83 a.u. when t_w is increased to 8 a.u. It is interesting that the 2-photon absorption has nearly equal population in $\ell = 0$ and 2 because the propensity to increase ℓ when a photon is absorbed would lead to the expectation that the $\ell = 2$ would be substantially larger.

In the $\ell = 0$ energy distribution, plotted in Fig. 2, there is large population corresponding to the two photon process where one photon is absorbed and one photon is emitted. This process is approximately 100× smaller for $\ell = 2$. This disparity is somewhat surprising considering that the two photon absorption probability is comparable. The propensity rule would lead to the expectation that $\ell = 0$ would be larger than the $\ell = 2$ but not by such a large factor. We attribute the $\ell = 0$ population to hole burning of the initial orbital. The coherent superposition of these Raman states with the initial state leads to a "hole" in the initial state at small r. Figure 3 shows the total probability ($\ell = 0$) in the Raman transition and in the two photon absorption as the pulse duration is increased keeping all other parameters fixed; the data in this figure comes from integrating the energy distribution up to $E = 0.875$ for the Raman transition and above $E = 0.875$ for the two photon absorption.[12] The dependence of the two photon absorption on t_w in Fig. 3 is the simplest to understand. The probability is approximately proportional to the duration because the ionization continues while the pulse is on. The behavior of the Raman population is more interesting, showing a slow increase followed by a decrease. The Raman popu-

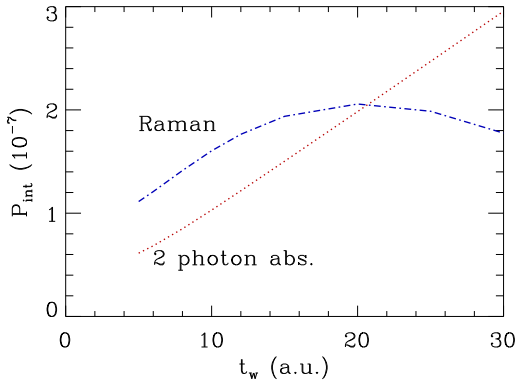

FIG. 3: The total probability to be in the $\ell = 0$ Raman structure (dash-dot line) or the $\ell = 0$ two photon absorption peak (dotted line). All laser parameters are as in Fig. 2 except for the pulse width, t_w, which is varied. The two photon absorption is approximately proportional to the duration of the laser pulse. The probability for Raman transition is not proportional to the pulse duration even for small t_w and begins to decrease when the bandwidth of the laser is too small to reach the $3s$, $4s$, ... states. As a point of comparison, $1/(E_{3s} - E_{2s}) \simeq 14$ a.u. For pulses longer than τ_{2s} the bandwidth becomes insufficient to reach the $3s$ state in a two photon Raman process.

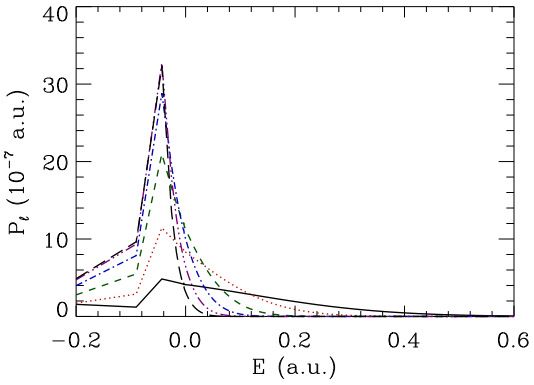

FIG. 4: Same as Fig. 2 but only for $\ell = 0$ and allowing t_w to vary as in Fig. 3: $t_w = 6$ a.u. (solid line), 10 a.u. (dotted line), 15 a.u. (dashed line), 20 a.u. (dash-dot line), 25 a.u. (dash-dot-dot-dot line), and 30 a.u. (long dash line). The longer duration gives a narrower energy distribution. The probability to be in the states nearest $n = 2$ increases with increasing duration until the band width of the laser becomes too narrow to reach those states.

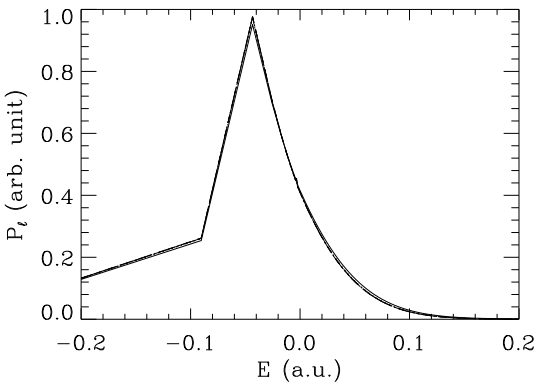

FIG. 5: Same as Fig. 4 but fixing $t_w = 18$ a.u. and allowing ω to vary. The integral of the curves have been fixed to be the same value. The curves are $\omega = 0.33$ a.u. (solid line), 0.67 a.u. (dotted line), 1.0 a.u. (dashed line), 1.33 a.u. (dash-dot line), 1.67 a.u. (dash-dot-dot-dot line), and 2.0 a.u. (long dash line). The lines are hardly distinguishable even though the total Raman probability decreases by more than 4 orders of magnitude from $\omega = 0.33$ to 2.0 a.u. This shows the shape of the energy distribution mainly depends on the laser duration and, hence, the shape of the hole does not strongly depend on the laser frequency.

lation starts decreasing when t_w is comparable to half the classical period; more specifically we find $t_w \sim \sqrt{8 \ln 2} n^3$. This condition is when the energy FWHM of the laser field equals $1/n^3$, i.e. the energy spacing of the atom. This fits with the interpretation of the Raman process with $\Delta\ell = 0$ as equivalent to hole burning. When the laser is on for a time comparable to or longer than the radial period for the hole in the wave function, then there should not be any hole burning.

Figure 4 shows how the energy distribution for $\ell = 0$ Raman transition changes as the pulse duration is increased keeping all other parameters fixed. One can see that the energy width is decreasing while the peak is increasing for longer t_w. However, the longest times have almost no increase in the peak while the width continues to decrease. At even larger t_w, the Raman population at all energies decreases until becoming approximately 0 when the bandwidth of the laser is too narrow to allow any change in energy. As with Fig. 2 population in individual states are hard to visualize. The population in the $1s$ state for each of the curves ($t_w = 6$ through 30 a.u.) is 1.46E-7, 3.95E-8, 1.08E-9, 4.35E-12, 1.87E-15, and 1.87E-19 while the population in the 3s state is 1.67E-8, 4.02E-8, 7.62E-8, 1.09E-7, 1.30E-7, and 1.34E-7.

Figure 5 shows how the energy distribution for $\ell = 0$ Raman transition changes as the *frequency* changes keeping the pulse duration at $t_w = 18$ a.u. The shape of the energy distribution is nearly the same for all frequencies shown even though there is a difference of more than four orders of magnitude in the total population. This fits with the interpretation of "hole burning" since the shape of the hole will mainly depend on the duration of the pulse and only weakly on the laser frequency; the Raman transitions arise from the projection of the hole in the initial wave function onto neighboring states. We note that the central energy of the 2-photon absorption peak shifts by $\sim 5/3$ a.u. for the same range of frequen-

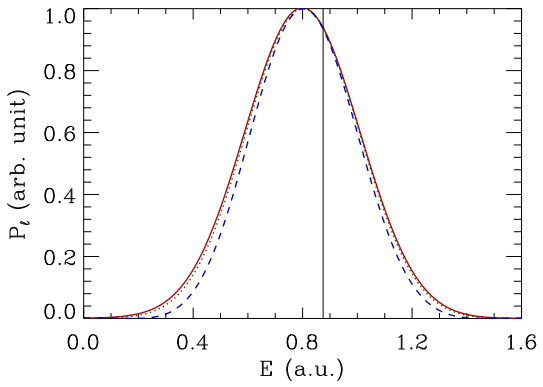

FIG. 6: Same as Fig. 2 but for $\ell = 1$ and allowing F_{max} to vary; the graph shows $F_{max} = 0.2$ (solid line), 0.4 (dotted line) and 0.8 a.u. (dashed line). The maximum value has been set to 1 for all curves. The energy distribution for the highest laser intensity is narrower and is slightly shifted to higher energies. The vertical line marks the energy $E_{init} + \omega$ where a narrow band laser would give the one-photon ionization.

cies shown in Fig. 5.

We performed calculations for other single valence atoms and found similar results. An exception is when the single photon transition is at a Cooper minimum. The single photon ionization is strongly suppressed in this situation while the two photon absorption is enhanced compared to the Raman transition.

IV. ONE PHOTON/THREE PHOTON IONIZATION

The "hole burning" can affect the one photon absorption process by changing the time when the electron is ionized and by changing the energy distribution near the one photon absorption peak. Within a perturbative picture, these effects result from the interference between one photon absorption and a three photon process (absorb-emit-absorb). The effect of "hole burning" should be to delay the photon absorption because the wave function is being depleted near the nucleus which is where photoabsorption takes place; the photoabsorption is delayed for strong laser fields because the electron probability near the nucleus needs to refill which requires time. Unlike the Raman process which is present even for weak laser fields, this effect should only become apparent at higher laser intensity reflecting a substantial change in the wave function.

For this section, we fixed the duration, $t_w = 6$ a.u., and frequency, $\omega = 1$ a.u., of the laser pulse. In all calculations, we started from the $2s$ state of hydrogen. The general trends did not depend strongly on the type of atom or initial state.

Figure 6 shows the energy distribution for $\ell = 1$ near the one photon absorption peak for $F_{max} = 0.2$, 0.4 and 0.8 a.u. These fields correspond to intensities of 1.4×10^{15}, 5.6×10^{15}, and 2.2×10^{16} W/cm^2. The maxima have been scaled to equal 1 for all F_{max}. As with the two photon absorption peak in Fig. 2, the position of the peak, $\simeq 0.8$ a.u., is slightly shifted to lower energy compared to the expected value: $1 - 1/8 = 0.875$ a.u. which is marked by a vertical line. The explanation of the shift is the same: the dipole transition matrix element is a decreasing function of energy. While the smaller F_{max} have nearly the same shape, the energy distribution is narrower and shifted slightly higher for the $F_{max} = 0.8$ a.u. case. This effect must be due to the interference between one photon absorption and a three photon process (either emit-absorb-absorb or absorb-emit-absorb or absorb-absorb-emit). By scaling all curves to have a peak of 1, we are hiding the fact that the energy distribution increases with laser intensity. However, we did not find that the increase was proportional to the laser intensity: the ratio of scaling factors for the highest and lowest intensities was 12 instead of 16 which is expected from perturbation theory.

As a point of comparison for the largest F_{max}, we compared other processes to that shown in Fig. 6. The p-wave three photon absorption is 240 times smaller. The f-wave energy distribution is approximately a 1000 times smaller for three photon absorption and of 2000 times smaller for the f-wave peak near 0.8 a.u. These small values might be surprising compared to the large non-perturbative character for the "one-photon" peak (e.g. the one-photon absorption was approximately 25% too small at $F_{max} = 0.8$ a.u.). However, it must be remembered that the three photon processes can interfere with the one photon process which can lead to a larger effect: the probability for an effect arising from interference of one- and three-photon transitions is $P = |A_1 + A_3|^2 = |A_1|^2 + (A_1 A_3^* + A_1^* A_3) + |A_3|^2$. The interference term is proportional to the square of the laser intensity while pure three-photon processes are proportional to the cube of the laser intensity. We note that the energy spread for the 3-photon absorption peak is $\sim 50\%$ broader than the 1-photon peak; the extra broadness arises because the higher order process depend on higher powers of the intensity and, thus, they appear to be effectively shorter in duration. A simplistic argument would suggest that the 1 photon peak would get broader at higher intensity because of the addition of 3 photon character. The narrowing we actually observe must be due to interference.

Figure 7 shows the time dependent current at $r = 50$ a.u. with the peak of the current scaled to be 1. A simple estimate of when the current should peak is $t_{peak} \sim 50/\sqrt{2E} = 39.5$ a.u. $\simeq 953$ as. The actual peak is somewhat earlier in time because the $-1/r$ potential gives a higher radial speed to the electron; a classical electron with energy 0.8 a.u. requires 907 as to reach 50 a.u. As in Fig. 6, the smaller intensities give similar results while the highest intensity gives a clear change. Part of the change is the current due to two-photon absorption which leads to higher energy electrons and a peak at early

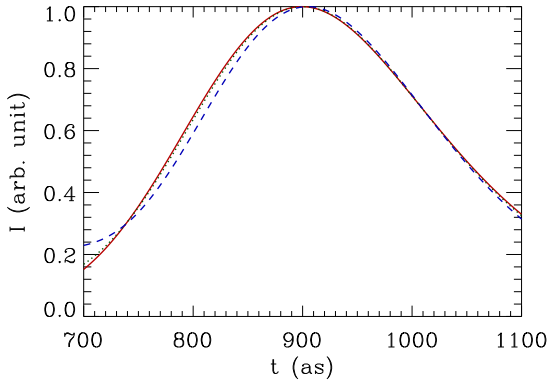

FIG. 7: The electron current at $r = 50$ a.u. from all angular momenta; the line types have the same meaning as Fig. 6. All the times shown are after the laser field is off. Note that the current at the highest intensity has slightly shifted to later times which agrees with the expectation of changes due to "hole burning".

times; in a similar vein, there is a slow decay at the highest intensity due to the Raman process which gives low energy electrons that reach $r = 50$ a.u. at later times. A more interesting effect is that the one photon peak is delayed by $\simeq 6$ as. Quantum mechanically this effect is due to the interference between one- and three-photon paths. Physically, the effect is consistent with the expectation of a time delay due to hole burning in the wave function.

We note that the interference between one- and two-photon processes in a single attosecond absorption has been discussed for both energy and angular distributions. Reference [14] discussed the effect on electron asymmetries, Ref. [15] discussed the effect on momentum and energy distributions and Ref. [16] gave an analysis based on perturbation theory. In our Fig. 2, one can see that the one photon absorption peak which falls between the Raman and 2-photon absorption peak would overlap them in energy. This would lead to left/right asymmetries in the electron angular distribution as discussed in Ref. [14].

V. CONCLUSIONS

We have performed calculations of attosecond absorption in one electron systems to explore some of the possible two- and three-photon effects. Our calculations demonstrate that one of the main two-photon effects is a Raman type process that leads to a strong redistribution of population with the same angular momentum as the initial state. We expect this process to be common and is related to "hole burning" of the initial wave function. The calculations also show that the interference of one- and three-photon paths can lead to changes substantially larger than might be expected. We argued that the time delay in the one-photon absorption with increasing laser intensity is also due to "hole burning" of the wave function.[7] Because the absorption mainly occurs near the nucleus, a hole there will decrease the ionization rate and lead to a delay of the photoabsorption.

In this paper, we focused on the hole burning in a one electron system. There can be other types of hole burning in two (or more) electron systems. An example involving a short range perturber coupled to a Rydberg series was investigated using the Ba $6snd\ ^{1,3}D_2$ states perturbed by the $5d7d\ ^1D_2$ state as the example.[8, 13] As an example requiring attosecond lasers, the Be ground state is nominally $2s^2$ in the valence shell. Calculations that include correlation have found that there is a large admixture of $2p^2$ in the ground state wave function. Typically, the photo-ionization is different from $2s$ and $2p$ orbitals. This leads to the possibility of having a hole burned in the radial coordinate (as described above) and a hole burned in the correlation. This will lead to substantial Raman transition to the nominally $2p^2$ autoionizing state. Thus, other types of wave packets can be initiated using hole burning.

This work was supported by the Chemical Sciences, Geosciences, and Biosciences Division of the Office of Basic Energy Sciencs, U.S. Department of Energy and by NWO. We acknowledge support from the EU Marie Curie ITN COHERENCE Network.

[1] P.M. Paul et al, Science **292**, 1689 (2001).
[2] M. Schultze et al, Science **328**, 1658 (2010).
[3] K. Klunder, et al, Phys. Rev. Lett. **106**, 143002 (2011).
[4] D. Guenot, et al, Phys. Rev. A **85**, 053424 (2012).
[5] S. Nagele, R. Pazourek, J. Feist, and J. Burgdorfer, Phys. Rev. A **85**, 033401 (2012).
[6] This result is derived by setting the radial momentum for angular momentum $\ell + 1$ and energy $E_{gnd} + \omega$ equal to the initial radial momentum.
[7] J.H. Hoogenraad, R.B. Vrijen, and L.D. Noordam, Phys. Rev. A **50**, 4133 (1994).
[8] D.I. Duncan and R.R. Jones, Phys. Rev. A **53**, 4338 (1996).
[9] L.D. Noordam H. Stapelfeldt, D.I. Duncan , T.F. Gallagher, Phys. Rev. Lett. **68**, 1496 (1992).
[10] T. Topcu and F. Robicheaux, J. Phys. B **40**, 1925 (2007).
[11] F. Robicheaux, J. Phys. B **45**, 135007 (2012).
[12] The way we grouped the Raman and 2-photon absorption is not accurate for t_w smaller than the data shown because the 2-photon absorption begins to have probability below $E = 0.875$ and the Raman transition has probability above $E = 0.875$.
[13] R.B. Vrijen, J.H. Hoogenraad, and L.D. Noordam, Phys. Rev. A **52**, 2279 (1995).
[14] L.-Y. Peng, F. Tan, Q. Gong, E.A. Pronin, and A.F. Starace, Phys. Rev. A **80**, 013407 (2009).
[15] L.-Y. Peng, E.A. Pronin, and A.F. Starace, New J. Phys. **10**, 025030 (2008).

[16] E.A. Pronin, A.F. Starace, M.V. Frolov, and N.L. Manakov, Phys. Rev. A **80**, 063403 (2009).